PHILOSOPHICAL TRANSACTIONS B

royalsocietypublishing.org/journal/rstb

Research

Cite this article: Liu W, Athreya S, Xing S, Wu X. 2022 Hominin evolution and diversity: a comparison of earlier-Middle and later-Middle Pleistocene hominin fossil variation in China. *Phil. Trans. R. Soc. B* **377**: 20210040.
https://doi.org/10.1098/rstb.2021.0040

Received: 13 April 2021
Accepted: 20 July 2021

One contribution of 11 to a theme issue 'The impact of Chinese palaeontology on evolutionary research'.

Subject Areas:
evolution

Keywords:
Middle Pleistocene, China, craniodental morphology, diversity

Authors for correspondence:
Wu Liu
e-mail: liuwu@ivpp.ac.cn
Sheela Athreya
e-mail: athreya@tamu.edu

Electronic supplementary material is available online at https://doi.org/10.6084/m9.figshare.c.5772140.

THE ROYAL SOCIETY PUBLISHING

Hominin evolution and diversity: a comparison of earlier-Middle and later-Middle Pleistocene hominin fossil variation in China

Wu Liu[1,2], Sheela Athreya[3], Song Xing[1,2] and Xiujie Wu[1,2]

[1]Laboratory of Vertebrate Evolution and Human Origins, Institute of Vertebrate Paleontology and Paleoanthropology, Chinese Academy of Sciences, Beijing 100044, People's Republic of China
[2]CAS Center for Excellence in Life and Paleoenvironment, Beijing 100044, People's Republic of China
[3]Liberal Arts Program, Texas A&M University-Qatar, Doha, Qatar

WL, 0000-0002-8444-368X; SX, 0000-0003-3069-4376; XW, 0000-0002-2893-9699

Historical views of Asia as an evolutionary 'backwater' are associated with the idea that *Homo erectus* experienced long periods of stasis and ultimately went extinct. However, recent discoveries of well-dated Middle Pleistocene hominin fossils in China have considerably challenged these ideas and provide sufficient data to propose a testable model that explains the patterning of variation in Middle Pleistocene China, and why it changed over time. A series of hominin fossil studies comparing earlier-Middle and later-Middle Pleistocene groups confirm that the expressions of certain traits shift around 300 ka. Fossils from the later Middle Pleistocene are more variable with a mix of archaic traits as well as ones that are common in Western Eurasian early *Homo sapiens* and Neanderthals. The period around 300 ka appears to have been a critical turning point for later-Middle Pleistocene morphological changes in China. It coincides with a phase of climatic instability in the Northern Hemisphere between Marine Isotope Stages 12 and 10 that would have led to changes in gene flow patterning, and regional population survival/extinction. This localized and testable model can be used for future explorations of hominin evolution in later Pleistocene eastern Eurasia.

This article is part of the theme issue 'The impact of Chinese palaeontology on evolutionary research'.

1. Introduction

The first hominin fossil discoveries in China were at the Zhoukoudian (ZKD) site in the 1920s. For decades they formed the single largest sample, and thus the primary body of paleoanthropological evidence for mainland East Asia. Cranial, mandibular and dental morphological patterns identified there were used to establish the defining features of Asian *Homo erectus* [1–6]. These fossils also dictated interpretations regarding later-Middle Pleistocene *Homo* evolution [7–9]. The predominant narrative for the past four decades has held that *H. erectus* was characterized by both evolutionary and cultural stasis and was an 'evolutionary dead-end' in Asia [10–13]. A less popular alternative model of regional continuity was also proposed for hominin evolution in East Asia [14–17]. However, owing to the outsized influence of the ZKD sample, both models overlooked the complex patterns of synchronic and diachronic variation within eastern Eurasia during the Middle Pleistocene [18,19].

In the past decades, more than 20 Middle Pleistocene (780–128 000 years ago/ka) sites have been identified in China [20,21]. New data that have emerged from recent excavations, dating improvements and fossil studies over the last 10 years [9,22–27] allow for a detailed analysis of evolutionary trends there during this critical period of evolution, which saw the disappearance of *H. erectus* morphology and the appearance of *Homo sapiens* elsewhere in

the world. These specimens are not easily allocated to existing taxonomic groups and reveal that populations in Middle Pleistocene China were highly variable after the period of around 300 ka. This evolutionary diversity is true even when an expanded *H. erectus* sample beyond the ZKD site is considered. Here we explore the patterns and possible reasons for the variability. The goal is to construct a testable model to explain the evolutionary processes that shaped hominin variation in eastern Eurasia from the early to the later Middle Pleistocene and go beyond the outdated models of the 1980s.

2. Background

The first Western models for human evolution that were specific to China were built primarily on archaeological data (e.g. [28–30]). Based on the presumed correlation between handaxes and cognitive evolution [31,32], scholars characterized the region relative to stereotypes that were consistently held about China by the West: that it was insular and slow to change [33]. Weidenreich was influential in amplifying Chinese anthropologists' more nuanced framework of evolution in the region, interpreting similarities between the ZKD crania and living East Asians as an indication of evolutionary links between the two [14], but these still treated the ZKD sample as characteristic of all *H. erectus*. Between the 1950s and 1970s, a steady programme of excavation and fossil studies by Chinese scholars enabled Wu & Zhang [15] to construct an updated model of regional evolutionary continuity, holding that morphological trends in geographical 'edges' (versus evolutionary 'centres') reflected continuity with gene flow from elsewhere in Eurasia [17,34]. However, the idea of evolutionary 'stasis' in Asian *H. erectus* has persisted [5,12].

Some recent studies have moved beyond these early ideas to investigate intra- and inter-regional patterns of *H. erectus* variation across East and Southeast Asia [5,6,35,36]. The best example of this is a detailed analysis of diachronic change in Indonesian *H. erectus* that recognizes temporal variation in Java and interprets it within a local ecological and evolutionary framework. This kind of study offers a significant improvement in our understanding of the complex factors that have shaped Pleistocene *Homo* there [37].

The increased sample of nearly complete and well-dated Middle Pleistocene crania in China, the application of new analytical tools such as high-resolution computed-tomography (CT) scanning, and improvements in chronometric dating of well-known samples have allowed for more refined observations of temporal and regional variation to be made. It is now clear that later Middle Pleistocene specimens including Dali, Jinniushan, Chaoxian, Maba, Xujiayao, Xuchang, Panxian Dadong and Tongzi do not follow the pattern of classical *H. erectus*, showing derived traits aligned with East Asian *H. sapiens* [7,22,23,27,38,39] and Neanderthals [26,40], while newer specimens such as Xuchang and Hualongdong possess novel morphologies for this time period and region [9,26]. It is also clear that following 300 ka there is a notable increase in craniodental variation and the appearance of novel traits [41].

The increase in morphological variability among Middle Pleistocene Chinese hominins coincides with a period of abrupt climatic changes in China between Marine Isotope Stages (MIS) 12–10, approximately 500–340 ka [42]. One of the largest amplitude changes in climate in the last 6 million years occurred between MIS 12–11. The MIS 11 interglacial was characterized by millennial-scale oscillations, particularly in the Northern Hemisphere, and was a significantly unstable period in northwestern China [43,44]. Both of these climatic conditions—warming and instability—have historically been associated with population movements [45–47], and models linking hominin variability to climatic instability have been proposed for Middle Pleistocene Europe [48] and for eastern Eurasia and Africa, particularly with respect to lineage diversification [49].

The goal of this study is to examine morphological variation between earlier- and later-Middle Pleistocene Chinese hominins (pre- and post-300 ka) and to explore possible palaeoclimatic correlates that could have contributed to this variation owing to a shift in evolutionary processes during this climatically unstable period. While we recognize that correlation does not equal causation, this study is an important first step in constructing a testable hypothesis and an interpretive framework for understanding variation in the Chinese Middle Pleistocene fossil record, and in particular how and why morphological patterns shifted from the earlier to the later periods. We conduct preliminary analyses of metric and nonmetric craniodental morphology to achieve a broad understanding of variation patterns in this regional and temporal sample. We then invoke palaeoclimatic data to construct a testable model of hominin evolution for present day China that is specific to the Middle Pleistocene.

3. Material and methods

(a) Sample and specimens

We looked at both metric and nonmetric data to analyse patterns of variation among specimens historically classified as *H. erectus*, and those with ambiguous affinities such as Dali, Jinniushan and Xujiayao (table 1). For the neurocranial metric analyses we examined 14 specimens that constitute every reasonably complete non-pathological Middle Pleistocene adult cranium from China (listed in the electronic supplementary material, table S1). For the dental specimens, both isolated teeth and those with maxillae and mandibles were used. All fossil teeth were scanned using a micro-CT to extract enamel-dentine junction (EDJ) morphology. The specimens were divided into two groups relevant to the question of a morphological pattern-shift during this time period. The earlier-Middle Pleistocene (earlier MP) group consists of Chinese specimens dated to pre-400 ka and the later-Middle Pleistocene (later MP) group comprises fossils younger than 300 ka. The temporal gap between these categories corresponds to the absence of fossils in China dating between 400–300 ka. The earlier MP group have been all recognized as *H. erectus*, while the later MP specimens are taxonomically ambiguous and may not even belong to the same species—a possibility that is premature to assume here but will merit further investigation. For the purposes of this study, we focus only on temporal patterns between the earlier Middle Pleistocene and the later Middle Pleistocene to address the assumption of stasis or homogeneity within Middle Pleistocene China.

(b) Data collection and analysis

We collected 25 linear neurocranial and seven facial measurements from original specimens, high-quality casts, and published descriptions of Chinese Middle Pleistocene fossils, plus six neurocranial indices, four facial indices and two angular measurements as well as cranial capacities (table 1 and table 2; electronic supplementary material, tables S1 and S2). The standard anthropological protocols of Martin [75] and Howells [76] were followed.

Table 1. The Middle Pleistocene hominin fossils used in the present study.

site	anatomical elements studied	geological age (Ma)	data source references
earlier-Middle Pleistocene (MP) group			
Zhoukoudian	crania (ZKD 2, ZKD 3, ZKD 5, ZKD 10, ZKD 11, ZKD 12)[b,c], mandibles[a,b,c], teeth[a,b,c]	0.5–0.78	[1–3,50,51]
Lantian Chenjiawo	mandibles[a,c], teeth[a]	0.65	[52]
Yiyuan	cranium[a], teeth[a]	0.63	[53,54]
Hexian	cranium[a,c], mandible[a,c], teeth[a,b]	0.412	[8,24,55,56]
Nanjing	cranium[b,c]	0.62–0.58	[57,58]
later-Middle Pleistocene (MP) group			
Dali	cranium[b,c]	0.3–0.26	[7,59,60]
Jinniushan	cranium[b,c]	0.26	[61,62]
Maba	cranium[a,b,c]	0.13–0.3	[39,63,64]
Changyang	maxilla[a,c]	0.195	[65,66]
Tongzi	teeth[a,c]	0.113–0.206	[27,67]
Chaoxian	cranium[a], teeth[a,c]	0.2–0.3	[38,66,68]
Dingcun	teeth[a,c]	0.16–0.2	[69]
Xujiayao	crania[a,b], mandible[a,c], teeth[a,c]	0.16–0.2	[23,66,69–73]
Panxian Dadong	teeth[a,c]	0.28–0.13	[22,74]
Xuchang 1	cranium[a,b,c]	0.125–0.105	[26]
Hualongdong 6	cranium[a,b,c], mandibles[a,c], teeth[a,c]	0.27–0.3	[9]

[a]Original fossil.
[b]Casts.
[c]Literatures.

Variance between the two fossil groups was explored using a multivariate analysis of variance (MANOVA). We performed multiple imputation and expectation-maximization [77–79] to impute missing variables on the raw data, and Darroch and Mossiman's method [80] to size-standardize them. Both raw and size-standardized data were used in all analyses. In order to avoid having more variables than observations in the MANOVA, we could not analyse more than 13 variables at a time. We, therefore, analysed the variables in five subsets (electronic supplementary material, table S3) representing conventionally recognized aspects of the cranium—braincase; frontal, parietal and occipital regions and facial skeleton—with some variables represented in more than one subset given that the cranium is not a set of independent modules [81]. In this review we are strictly exploring variance in the two samples, not hypothesis testing using independent lines of evidence; so the presence of some variables in more than one subset is not providing a falsely positive result but rather allows us to explore covariation among various measurements of the cranium, and avoid two statistical problems: (i) risking a Type 1 error by performing several independent ANOVAs; and (ii) overdetermination due to having more predictors than observations. We examined the Wilk's Lambda and Levene's *F* statistics to assess the differences in variance between the two fossil groups, as well as the variance of individual variables within each group (electronic supplementary material, table S4). Our prediction is that the variance will be consistently higher in the later MP group, so we used one-tailed test with a significance level of 0.10.

The multivariate analysis was performed with principal component analysis (PCA). In order to maximize the number of specimens for inclusion in PCA analyses, we used seven variables (biparietal breadth (BPB), minimum frontal breadth (WFB), maximum frontal breadth (XFB), parietal sagittal chord (PAC), parietal subtense (PAS), maximum breadth of supraorbital torus wings (XSOT) and supraorbital torus thickness-middle (SOTT-middle)). Parietal arc was excluded to avoid redundancy with parietal chord. PCA was computed on the correlation matrix to standardize variation. Finally, we compared coefficients of variation, ratio measurements, and nonmetric traits to develop an overall sense of morphological patterns within the earlier MP and later MP groups. Statistics were performed with PAST v. 3.0 and SPSS v. 20.0.

4. Results

(a) Univariate and multivariate analyses

In the MANOVA, variables capturing overall neurocranial shape (see the electronic supplementary material, tables S3 and S4) are significantly different between the earlier MP versus later MP sample in both raw and size-standardized analyses. In the raw data, 16 variables have significantly higher variances in the later sample while in the size-standardized data, six variables have a higher variance.

The PCA reveals a morphological space characterized by only one dominant component, which explains 68.1% of the variance (electronic supplementary material, table S5). The second component explains 18.0% of the variance (figure 1). It is above the Jolliffe threshold value (Jolliffe cut-off: 0.7), but not above the broken stick model of random variation. Hence, its reliability must be considered with caution. The following components explain less than 13.9% of the variance, and they will not be considered here. PC1 is a size vector, associated with an increase of all the variables

Table 2. Means and s.d. of linear measurements (mm), index, occipital angle (°) and cranial capacity (cm^3) of earlier- and later-Middle Pleistocene hominins in China (without imputation of missing data).

measurements	earlier-Middle Pleistocene group (mean ± s.d.)	later-Middle Pleistocene group (mean ± s.d.)
maximum cranial length (GOL)	194.0 ± 9.46 ($n = 8$)	209.5 ± 5.63 ($n = 3$)
maximum cranial breadth (XCB)	149.6 ± 6.72 ($n = 7$)	158.1 ± 14.91 ($n = 5$)
biparietal breadth (BPB)	137.9 ± 4.73 ($n = 8$)	152.3 ± 11.67 ($n = 6$)
minimum frontal breadth (WFB)	86.9 ± 5.58 ($n = 8$)	108.3 ± 10.28 ($n = 5$)
maximum frontal breadth (XFB)	108.9 ± 6.66 ($n = 8$)	128.8 ± 10.1 ($n = 6$)
biasterion breadth (ASB)	116.2 ± 9.73 ($n = 8$)	124.0 ± 9.13 ($n = 5$)
auricular vertex height (AVH)	96.0 ± 4.71 ($n = 7$)	103.3 ± 2.84 ($n = 5$)
auricular-bregma height (ABH)	93.0 ± 3.93 ($n = 7$)	99.2 ± 1.87 ($n = 5$)
frontal sagittal arc (FRA)	121.0 ± 8.94 ($n = 8$)	128.4 ± 10.66 ($n = 4$)
frontal sagittal chord (FRC)	107.4 ± 8.60 ($n = 8$)	109.4 ± 7.86 ($n = 4$)
parietal sagittal arc (PAA)	102.0 ± 8.59 ($n = 8$)	115.8 ± 7.63 ($n = 6$)
parital sagittal chord (PAC)	96.5 ± 8.00 ($n = 8$)	107.5 ± 7.23 ($n = 6$)
parietal subtense (PAS)	14.3 ± 2.30 ($n = 8$)	18.96 ± 2.43 ($n = 6$)
lambda-asterion arc (LAA)	88.6 ± 7.05 ($n = 8$)	99.5 ± 12.64 ($n = 4$)
lambda-asterion chord (LAC)	81.5 ± 5.04 ($n = 8$)	92.2 ± 10.68 ($n = 4$)
lambda-inion arc (LIA)	50.8 ± 3.82 ($n = 6$)	77.6 ± 11.97 ($n = 4$)
lambda-inion chord (LIC)	48.3 ± 2.84 ($n = 7$)	69.7 ± 12.08 ($n = 4$)
bregma-asterion arc (BAA)	145.1 ± 7.80 ($n = 8$)	170.0 ± 14.52 ($n = 4$)
bregma-asterion chord (BAC)	126.1 ± 5.00 ($n = 8$)	140.3 ± 12.69 ($n = 4$)
temporal squama height (TEMPSQHT)	37.9 ± 3.23 ($n = 7$)	45.1 ± 2.83 ($n = 4$)
thickness at parietal tuber (THPE)	10.6 ± 1.47 ($n = 7$)	8.37 ± 2.20 ($n = 6$)
supraobital torus thickness-middle (SOTT-middle)	13.8 ± 2.63 ($n = 8$)	14.4 ± 4.79 ($n = 5$)
supraobital torus thickness-medial (SOTT-medial)	15.1 ± 2.71 ($n = 8$)	16.0 ± 1.44 ($n = 4$)
supraorbital torus thickness-lateral (SOTT-lateral)	12.0 ± 1.39 ($n = 7$)	13.0 ± 1.36 ($n = 5$)
maximum breadth of supraorbital torus wings (XSOT)	112.7 ± 6.18 ($n = 8$)	129.4 ± 9.92 ($n = 5$)
bizygomatic breadth (ZYB)	145.0 ± 2.65 ($n = 3$)	144.5 ± 4.95 ($n = 2$)
upper facial height (NPH)	76.7 ± 4.51 ($n = 3$)	76.3 ± 2.91 ($n = 3$)
bimaxillary breadth (ZMB)	98.0 ($n = 1$)	109.2 ± 5.35 ($n = 3$)
orbit breadth (OBB)	41.1 ± 2.95 ($n = 3$)	46.1 ± 4.04 ($n = 4$)
orbit height (OBH)	34.5 ± 2.16 ($n = 3$)	37.2 ± 3.16 ($n = 4$)
nasal breadth (NLB)	30.9 ± 1.50 ($n = 3$)	31.3 ± 1.53 ($n = 3$)
nasal height (NLH)	54.7 ± 2.57 ($n = 3$)	56.1 ± 8.05 ($n = 3$)
cranial length-auricular height index (ABH/GOL)	48.0 ± 1.68 ($n = 8$)	47.7 ± 1.99 ($n = 4$)
cranial breadth-auricular height index (ABH/XCB)	62.2 ± 2.34 ($n = 8$)	63.1 ± 5.06 ($n = 6$)
frontal curvature index (FRC/FRA)	88.8 ± 2.92 ($n = 8$)	85.3 ± 1.81 ($n = 4$)
parietal curvature index (PAC/PAA)	94.6 ± 0.96 ($n = 8$)	92.9 ± 1.71 ($n = 6$)
occipital curvature index (LIC/LIA)	92.7 ± 5.93 ($n = 7$)	89.8 ± 7.07 ($n = 4$)
bregma-asterion index (BAC/BAA)	87.0 ± 2.78 ($n = 8$)	82.3 ± 2.18 ($n = 4$)
upper facial index (NPH/ZYB)	52.8 ± 3.33 ($n = 3$)	51.7 ± 2.19 ($n = 2$)
middle facial index (NPH/ZMB)	73.4 ($n = 1$)	70.0 ± 3.33 ($n = 3$)
orbit index (OBH/OBB)	84.2 ± 7.78 ($n = 3$)	81.3 ± 12.18 ($n = 4$)
nasal index (NLB/NLH)	56.5 ± 0.78 ($n = 3$)	56.8 ± 9.33 ($n = 3$)
occipital angle (°)	103.0 ± 4.36 ($n = 3$)	99.4 ± 7.99 ($n = 2$)
nasomalar angle (°)	143.9 ± 2.82 ($n = 4$)	144.7 ± 2.69 ($n = 3$)
cranial capacity (CC) (cm^3)	1032 ± 116.7 ($n = 8$)	1352 ± 273.6 ($n = 5$)

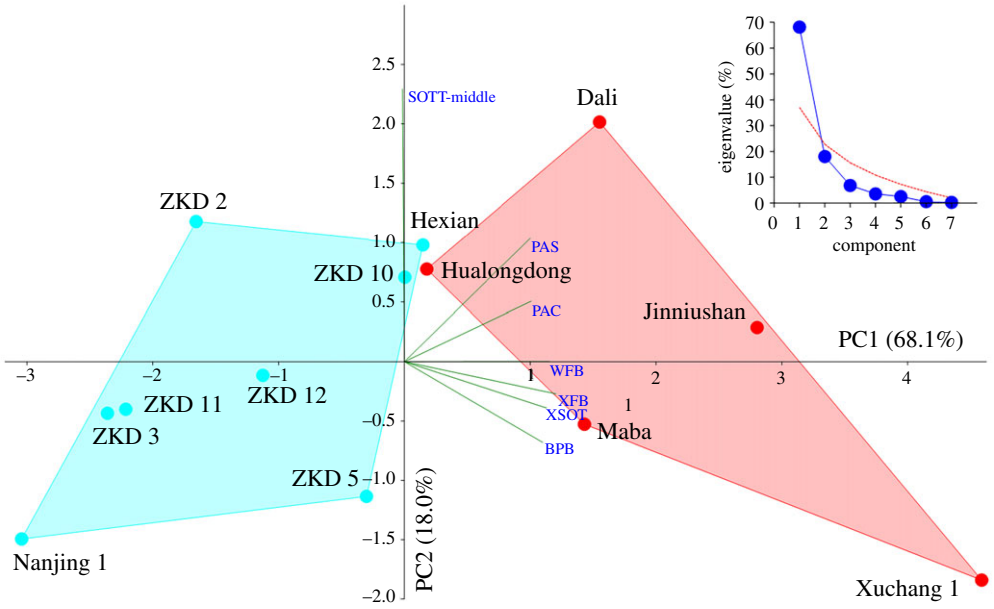

Figure 1. Principal component analysis showing the distribution of the two groups according to the first two principal components using seven variables. Right above: scree plot and broken stick level. (Online version in colour.)

except SOTT-middle. PC2 is associated with an increase of parietal length, parietal subtense, and supraorbital torus thickness, and decrease in width. Within this space, later MP group separated earlier MP group according to the large cranial dimension and thick supraorbital torus. The overlapping of cranial vault contours of some earlier and later Middle Pleistocene hominin crania from China provide similar result (figure 2).

(b) Neurocranial indices and nonmetric traits

Compared to the earlier MP fossils, the later MP sample has pronounced variation in the neurocranial vault, in particular the relationship between overall length and height (cranial length-auricular height index—ABH/GOL) (figure 3 and table 2). The earlier MP sample has a narrow range of variation in this ratio, with only the ZKD 5 specimen plotting as an outlier owing to its extremely long cranium. By contrast, the later MP group encompasses the extremes of the whole sample, with the Hualongdong 6 and Xujiayao 6 specimens possessing the highest ratios owing to their relatively short but extremely high crania, and the roughly contemporaneous Xuchang 1 fossil falling at the lowest end of the distribution and plotting with the ZKD 5 fossil owing to its long, low cranial vault (figure 1 and table 2).

The frontal curvature indices (FRC/FRA) between the two samples are significantly different ($p = 0.02$), with an average of 85.3 for the later MP sample versus 88.8 for the earlier fossils. The lower value reflects the more bulging frontal bones of the younger sample but again this is highly variable. When size-standardized frontal chord and arc values are examined, the Hualongdong, Xujiayao and Xuchang fossils cluster at the lowest end of the distribution with nearly equal lengths for both, while the Dali, Jinniushan, and Maba specimens have longer arcs relative to chords.

The parietal curvature index (PAC/PAA) is significantly different ($p = 0.02$) with the younger group possessing lower ratio values owing to the increase in arc relative to chord length. They possess longer parietal sagittal chords in absolute terms, but considerably shorter chords relative to arc in size-standardized measurements. This is a product of the absolute increase in brain size, but also the increased sagittal parietal curvature of the younger sample. The bregma-asterion chord and arc index (BAC/BAA) capture the posterior horizontal curvature of the neurocranium. When the data are size-standardized, the later MP fossils span the extremes of the entire study sample with Dali possessing the shortest BAC and one of the shortest BAA, and Xujiayao 6 having the longest BAA and BAC even when accounting for overall body size. In addition, the BAC/BAA ratio values are significantly smaller in the later versus earlier MP samples ($p = 0.01$) reflecting increased posterior parietal expansion. The BAC/BAA values for the later MP fossils fall within the range of Late Pleistocene hominins and are consistent with parietal expansion related to encephalization (figure 2) [26,60].

While the horizontal aspect of the neurocranium is more bulging in the younger sample, the occipital curvature index (LIC/LIA) is highly variable: Jinniushan's value of 82.0 is well below the entire sample range and reflects its bulging occipital sagittal profile, Dali's value of 85.8 in the low range of *H. erectus*, while the other later MP specimens from Xuchang 1 has a value of 94.4, respectively, which is within the *H. erectus* range.

A well-developed sagittal keel is typical among East Asian *H. erectus* and generally presents as a pronounced bulge that extends the length of the frontal and most of the parietal bone, with parasagittal depressions and a bregmatic eminence. These features are variably expressed in the later MP group. On the Dali specimen the keel is only on the frontal bone and it does not reach the weakly developed bregmatic eminence. Because of this, it has been considered a metopic versus a sagittal keel [60] (figure 4). On the younger specimens, Jinniushan and Hualongdong 6 in particular, the keel morphology follows the pattern seen in *H. erectus* but is more weakly expressed.

The position of the maximum cranial breadth is a diagnostic feature of *H. erectus*. It sits low on the cranium at the level of the supramastoid crest. In this study, the later MP fossils from China are similar to the earlier MP group in that the maximum breadth is located not superiorly on the

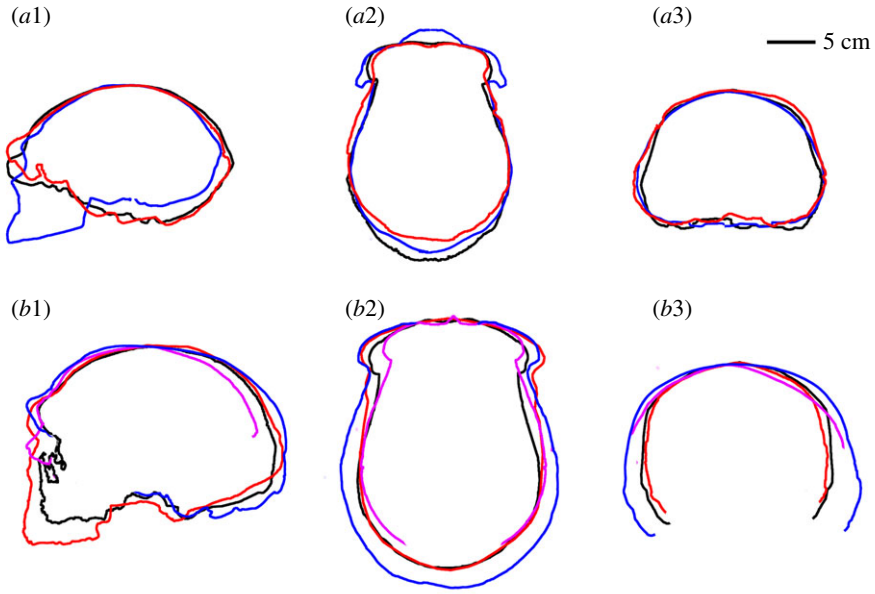

Figure 2. Overlap of cranial vault contours for the earlier Middle Pleistocene group (upper: ZKD (black), Hexian (red), Nanjing1 (blue)) and later Middle Pleistocene group (below: Dali (black), Jinniushan (red), Xuchang (blue), Maba (pink)).

parietals—as seen in later *Homo*—but more inferiorly, at the upper posterior temporal bone. However, in anterior and posterior views the later MP sample depart from the *H. erectus* pattern in that the parietal walls are not inclined in the same way. They rise almost vertically from the supramastoid region and become slightly inclined at different positions—more superiorly on Dali and Hualongdong, but inferiorly at the level of the mastoid crest on Jinniushan. These fossils also have variably present and prominent parietal eminences (figure 4). As noted earlier, the average reduction in the BAC/BAA index from 87.0 to 82.3 reflects the relative shortening of the chord versus arc which results from the increased posterior parietal curvature that accompanies encephalization in the later MP group (table 2).

(c) Facial skeleton

In the facial skeleton, the two temporal groups are not notably different (figure 4 and table 2; electronic supplementary material, table S2). The index of upper facial height to zygomatic width (NPH/ZYB) ranges from 50.0–56.5 in *H. erectus*, and in Dali and Jinniushan it is 53.2 and 50.1, respectively. Similarly, the index of upper facial height to mid-facial width (NPH/ZMB) is approximately similar. These two indices indicate that all Chinese Middle Pleistocene hominins have wide and low upper faces. The average nasomalar angle reflects upper face flatness with a higher angle resulting from a more flat upper face. It increases from a range of 140.3° to 147.2° in the earlier MP sample to between 143.0° and 147.8° in the later MP sample indicating a notably flat upper face.

The orbits of the earlier MP group are generally square-shaped with a mean orbit index (orbit height/breadth) of 84.2 which is owing to relatively high versus wide orbits. Of the later MP specimens with preserved orbital regions, Dali and Jinniushan have irregular-shaped orbits with curved upper borders and approximately horizontal lower borders, and indices below the *H. erectus* sample of 75.6 and 67.3, respectively. The orbits of Maba are circular or rounded which is clearly different from the square-shaped orbits of other Chinese Middle Pleistocene hominins. The newly discovered Hualongdong 6 cranium also has circular or curved upper and lower borders with an orbit index of 94.4 which exceeds all other Middle Pleistocene hominins [9] (figure 3).

In the nasal region, reconstructed crania of ZKD and Nanjing 1 were used since only a few Chinese *H. erectus* specimens have preserved facial bones. A mean nasal index of 56.5 was obtained for Chinese *H. erectus*. The nasal aperture in the later MP group is highly variable. On Dali, it is wide and low with a nasal index (nasal height/breadth) of 62.3, which is similar to Jinniushan with a nasal index of 62.0. Hualongdong 6 has a narrow and high nasal apertures with an index of 46.0 [9].

Middle Pleistocene hominins are characterized by pronounced supraorbital tori. Among the earlier and later Chinese, the two temporal groups show different morphological expressions of this trait. Chinese *H. erectus* are characterized by horizontal supraorbital torus with projecting glabella, with the thickest part of the torus in the medial portion of the supraciliary arch. The tori in the later MP group are much more variable. Hualongdong and Dali have glabellar depressions and robust and vertically thick tori like *H. erectus*, but with arches over each orbit, while Maba and Xuchang have gracile tori with slight arches that are medially thick and laterally thin, more similar to Neanderthals (figure 3). The torus of Jinniushan is much less developed but it has a glabellar projection and its thickest portion is medial, resembling the supraorbital tori of ZKD and Nanjing. Above the torus, the earlier MP sample has a deep supratoral sulcus while the later MP specimens have shallow supratoral sulci. The evolutionary or taxonomic value of supraorbital morphology is not clear [82] and it is not considered diagnostic in and of itself for Middle Pleistocene *Homo* [83,84], but the increased variability later in the Middle Pleistocene is apparent.

5. Dental morphology

Recent studies of dental remains from ZKD, Hexian and Yiyuan indicate that earlier-Middle Pleistocene hominins in

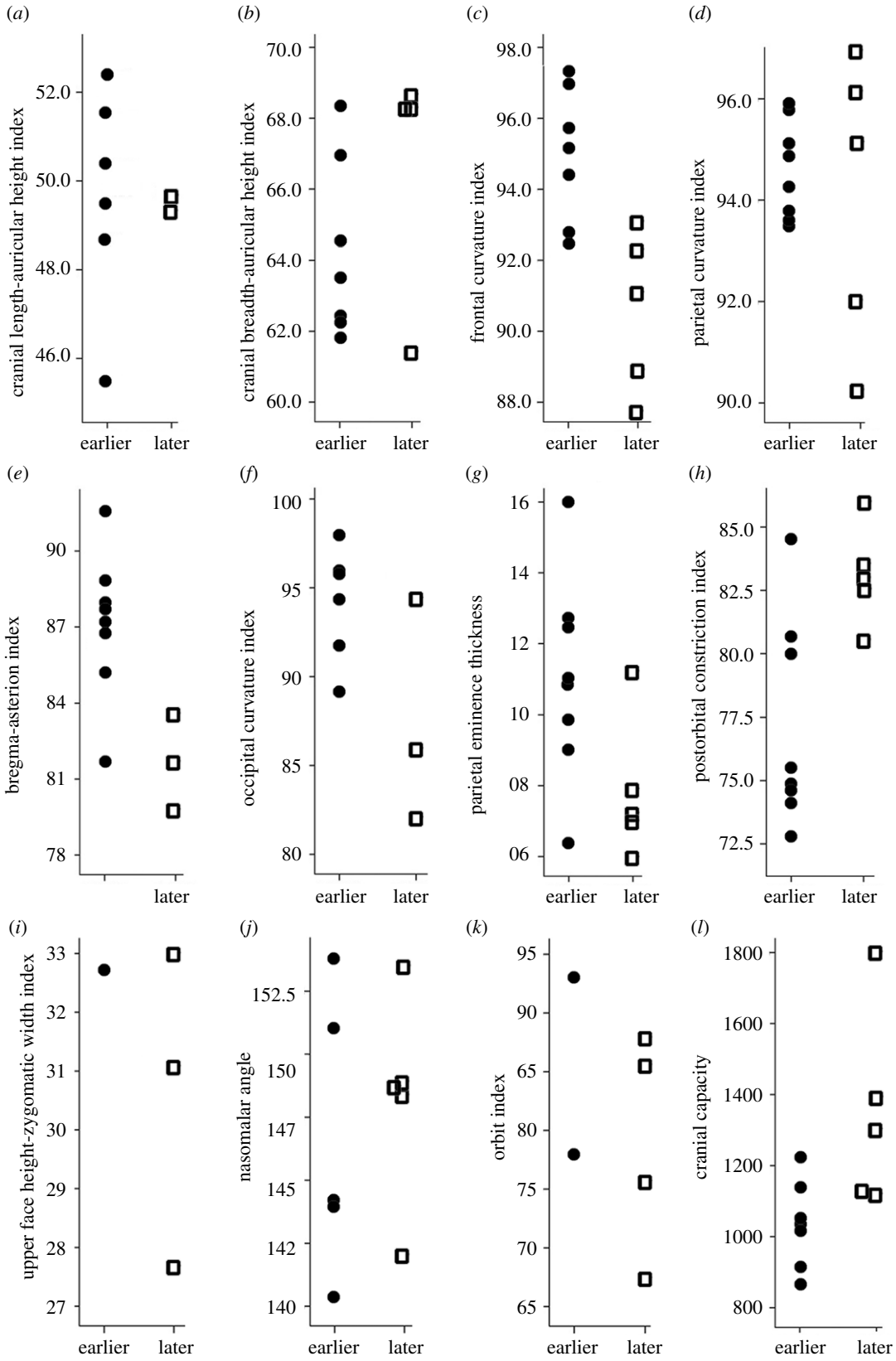

Figure 3. Distributions of selected cranial measurements and indices for earlier and later Middle Pleistocene group humans from China.

China are characterized by large dentition with robust crown and roots, complicated occlusal morphology and asymmetrical crown outlines in their molars and premolars [24,51,53]. The robust and complicated crown morphologies are mainly expressed as buttressing and accessory structures on the crown. These include basal tubercles and finger-like projections on the lingual side of the upper central incisors, bifurcation of the main occlusal and transverse crests on the premolars, vertical grooves on the buccal surface as well as asymmetrical crown outlines of premolars, the presence of a mesial accessary ridge on the maxillary molars, a deflecting wrinkle and the presence of cusps six and seven on the lower molars. The robust roots are expressed as pronounced furcation such as three rooted upper premolars. Most of these features were defined and described by Weidenreich [3] and can be observed more frequently in the teeth of Early

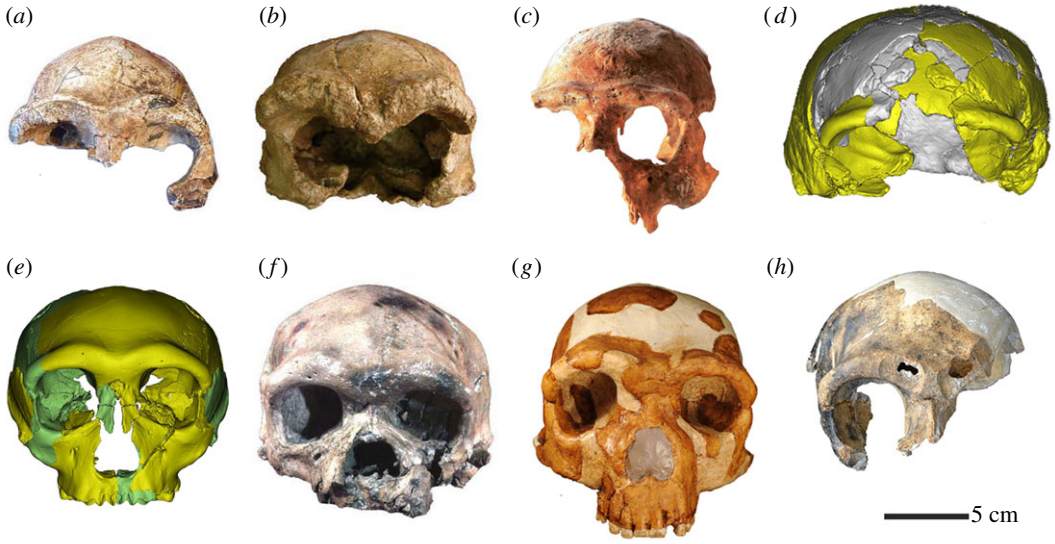

Figure 4. Anterior cranial profiles of Middle Pleistocene humans from China. (*a*) ZKD 12; (*b*) Hexian; (*c*) Nanjing; (*d*) Xuchang 1; (*e*) Hualongdong; (*f*) Dali; (*g*) Jinniushan; and H: Maba. (Online version in colour.)

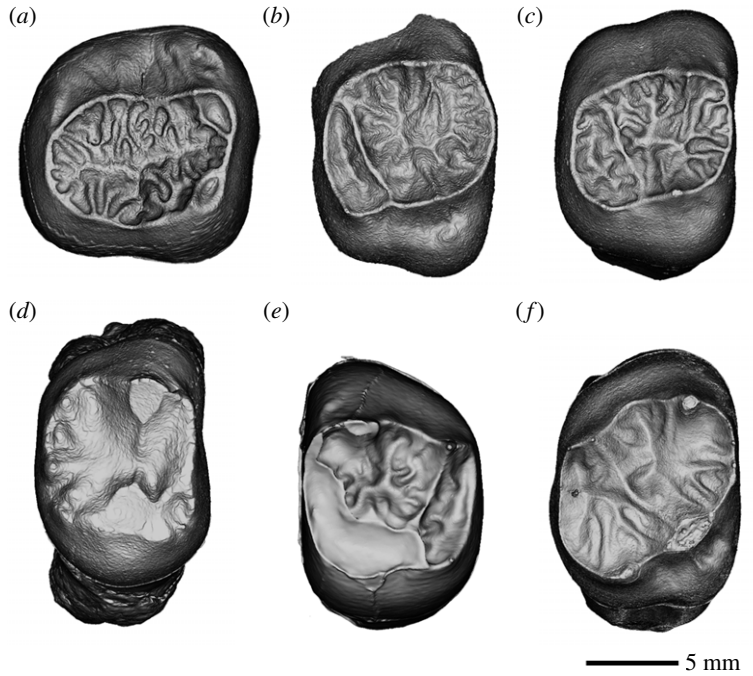

Figure 5. Dental morphologies at the EDJ surface of Middle Pleistocene hominins from China. (*a*) ZKD PA70 (left M_2); (*b*) Hexian PA837 (right M^2); (*c*) Yiyuan Sh.y.008 (right M^2); (*d*) Xujiayao PA1481 (right M^3); (*e*) Changyang PA76 (left M^1); and (*f*) Tongzi PA875 (right M^1).

and Middle Pleistocene hominins, and have been treated as primitive features characterizing *H. erectus* [3,51,53].

The EDJ surface of earlier-Middle Pleistocene hominins is complicated with pronounced furrows, ridges and accessory cusps, and in particular a vertical groove on the buccal side of both lower and upper premolars, Carabelli's cusp on the upper molars and the presence of a protostylid on the lower molars. The Carabelli's cusp and protostylid in the earlier MP group are usually pronounced with clear horizontal grooves or clefts, or a shelf-like lingual cingulum [24,51,53,85]. In addition, the EDJ surface of earlier group specimens is highly crenulated forming a 'dendrite-like' EDJ morphology (figure 5). So far, this special EDJ feature has only been found in the Chinese earlier-Middle Pleistocene hominins and may represent a derived feature specific to earlier-Middle Pleistocene East Asian *H. erectus* of [53].

The dental morphology of later-Middle Pleistocene hominins in China is simple and gracile in comparison to the earlier-Middle Pleistocene hominins. The later MP sample is characterized by small-sized teeth, and less complicated structures such as the absence of a basal tubercle, and a decrease in finger-like projections and secondary furrows and ridges. However, some recent studies on the teeth of Chaoxian, Panxian Dadong, Xujiayao and Tongzi from the later MP group indicate that the dental morphology of this time period exhibits much greater variability than in earlier-Middle Pleistocene hominins (22, 23, 27, 38). Compared with other specimens from the later MP group, the teeth of Chaoxian preserve more archaic features with larger teeth in size falling

within the range of variation of Chinese *H. erectus*. They also possess some typical *erectus*-like non-metric traits including well-developed accessory ridges in P^4, bifurcations of the main crests on the occlusal surface of P^3 and P^4, and accessory furrows and ridges on the occlusal surface of the molars [38]. Similarly, the Xujiayao teeth possess both *erectus*-like features as well as those frequently occurring in *H. sapiens* [23]. The teeth of Panxian Dadong exhibit more derived features than other later-Middle Pleistocene hominins. For example, the upper central incisor is robust with a pronounced basal tubercle, finger-like projections and marginal ridges on the lingual crown, while the other three teeth possess more features of early and recent modern humans in terms of crown outline and symmetry, tooth size and gracile morphology [22]. A recent study on the hominin teeth from the later-Middle Pleistocene Tongzi site reveals that the buccal width of the P^3crown exceeds that of the lingual side, a pattern that resembles Late Pleistocene *Homo* (Neanderthals and early modern *H. sapiens*) [27].

These dental morphological patterns among Chinese Middle Pleistocene hominins indicate that the specimens from the earlier MP group keep more primitive or common features shared by East Asian *H. erectus*. Most of these features, such as large dentition with robust crown and roots and complicated occlusal morphology, are either weakly expressed or absent in some later MP group specimens (Panxian Dadong). However, other later MP group specimens (Chaoxian and Xujiayo) still keep these primitive dental features. It is noteworthy that the dendrite-like EDJ morphology which reflect the development of specific or derived features for Chinese *H. erectus* was absent in the later MP group.

6. Discussion

(a) Variation, skull form and cranial capacity

It is well known that the earlier-to-later-Middle Pleistocene transition is characterized by a trend in encephalization among most Eurasian and African hominins [86–88]. In China, the average cranial capacity of the earlier MP specimens is 1032 cm^3 with ranges from 876–1225 cm^3 while in the later Middle Pleistocene the average increases to 1352 cm^3. Almost all later MP specimens have cranial capacities exceeding 1300 cm^3 with Xuchang's even reaching the remarkable figure of 1800 cm^3. The two exceptions are Dali and Hualongdong 6 which have cranial capacities of 1120 and 1150 cm^3, respectively. Table 3 provides the comparisons of cranial capacity and other selected cranial and dental features between earlier and later MP hominin groups in China.

(b) Morphological variation and climate change in the pleistocene

The central observation of this study is that morphological variability among hominin populations in China increased considerably after 300 ka. This is borne out by the findings of univariate and multivariate analyses and cannot be explained solely by either size differences or encephalization, although both of these factors are relevant and important sources of variation between the two samples. However, other evolutionary forces are known to shape morphological variation—namely, to increase variability—and should be considered here. First, Van Valen [89] long ago showed that the wider the niche, the greater the variability of a species or subspecies. Second, Kolbe *et al*. [90] confirm that differential admixture can lead to greater morphological variation between an established population and an incoming one. We combine this with the body of research that has demonstrated a strong correlation between hominin dispersals and climatic instability [45,91–93]. After the mid-Bruhnes event (*ca* 420 ka) it is known that both northern and southern China experienced more intense glacial–interglacial amplitudes with shorter intervals of between 23–100 kyr [43,94,95]. Ash & Gallup [92] studied the correlation between the encephalization quotients of 109 *Homo* crania and two climate proxies—sea surface temperature and oxygen isotope data ($\delta^{18}O$)—and found the strongest statistically significant correlations to be between cranial capacity and climatic data averaged over 100 kyr intervals (versus 200 kyr).

The newly reported 146 ka hominin cranium from Harbin, northeast China exhibits a combination of both primitive and derived characters [96]. In our opinion, this morphological pattern provides further support to the morphological and evolutionary diversity of the late Middle Pleistocene in present day China. Some features like nasal morphology should reflect climate adaptation.

Based on these lines of evidence, we hypothesize that the increased morphological variability in later-Middle Pleistocene Chinese hominins was shaped by climatic variability. Simply put, we hypothesize a causal relationship at the heart of this correlation with two mechanisms at play. First, the climatic instability may have led to population dispersals and admixture, and second—following Potts [97]—if variability selection was operating it would have favoured evolutionary processes that allowed for a wider range of responses to the periodic instability. This would include encephalization and the behavioural flexibility and advance planning preferred on hominins with more complex cerebral cortex wiring. Environmental instability, morphological variation and evolutionary change in mid-Pleistocene China may be intimately intertwined and should be the focus of further detailed studies of hominin evolution there.

(c) Implication on taxonomy

Recent hominin fossil discoveries plus additional work on dating and morphological studies of Xujiayao, Penghu, Xuchang and Xiahe have revealed not only complicated patterns of morphological diversity but different coexisting morphological patterns comprised primitive, derived or some individual-specific unique features [23,26,98–100]. With these findings, the possible coexistence of several hominin taxa including late archaic hominins, early modern humans, Denisovans and some unidentified group during the later Middle Pleistocene in China was proposed. The analyses of the present study provide further support to the morphological diversity of hominins in this time period although taxonomic implications for specific regional populations in later-Middle Pleistocene hominins of China are still not fully understood at the moment.

7. Conclusion

Weidenreich's study of the ZKD specimens [1–3] established that the crania, mandibles and teeth of *Sinanthropus* exhibited a suite of shared features that have contributed to the

Table 3. Comparison of cranial and dental features between earlier and later group specimens.

features	earlier-Middle Pleistocene group	later-Middle Pleistocene group
cranial capacity	860–1225 cm^3 with average of 1032 cm^3	more variable with average of 1352 cm^3, and maximum of 1800 cm^3 and minimum of 1120 cm^3
cranial thickness	thick	variable
cranial outline shape	pear or teardrop shaped in superior view; long and low in sagittal view	long with increased cranial height in sagittal view
position of maximum cranial breadth	sits at level of supramastoid crest	located at upper posterior temporal bone
sagittal keel	present with pronounced expression	weak or variable
orbital shape	square-shaped and relatively high	variable
supraorbital torus configuration	not divided into distinct medial and lateral portions; glabella is depressed relative to nasofrontal suture	divided into distinct medial and lateral portions; glabella is swollen relative to nasofrontal suture
postorbital constriction	yes	reduced relative to earlier group
frontal squama	flat with weak or variable keel and typically absent bregmatic eminence	short and arched with narrow, high frontal keel and separate bregmatic eminence
parietal	relatively short and flat with no bossing relative to bimastoid width	relatively short and arched with bossing of parietal walls and significant expansion of posterior parietal in the horizonal dimension
temporal squama contour	low and flat or weakly arched with pronounced lines	high and arched with weak lines
angular torus	present/pronounced	absent/variable
occipital versus nuchal plane	shorter or equal occipital to nuchal plane; sharp angle between the two	longer occipital to nuchal plane; moderate angle between the two
nasal aperture shape	high with mean nasal index of 56.5	variable
general dental morphological pattern	large dentition with robust crown and roots, complicated occlusal morphology, and asymmetrical crown outlines in their molars and premolars. The EDJ surface was complicated with pronounced furrows, ridges and accessory cusps, and in particular a vertical groove on the buccal side of both lower and upper premolars	the dental morphologies are characterized by small-sized teeth, less complicated structures (such as the absence of a basal tubercle, and a decrease in finger-like projections and secondary furrows and ridges). The morphology of EDJ surface is simple
'dendrite-like' EDJ	the EDJ surface is highly crenulated forming a 'dendrite-like' EDJ morphology	not present
variability in dental morphology	the dental morphologies in the earlier group specimens are less variable	exhibiting much greater variability than the teeth of early Middle Pleistocene hominins. Both Chaoxian and Xujiayao teeth exhibit a series erectus-like features. By contrast, the teeth of Panxian Dadong and Hualongdong possess more features of modern humans

perception that East Asian *H. erectus* was relatively homogeneous and evolutionarily stagnant [5,55,58]. An expanded fossil record for Middle Pleistocene China provides a more nuanced understanding of hominins of this time. Using non-metric features and metric analyses we explored (i) whether the *degree* of craniodental variation was higher in the later MP versus earlier MP group; and (ii) whether this increased variability could be linked to climatic instability or change.

Analyses confirm that the answer to the first question is yes; and this reveals an important point about hominin evolution in Middle Pleistocene China. Late Middle Pleistocene *Homo* in China is characterized not by a particular suite of traits but rather by a pattern of increased morphological variability. Although several *erectus*-like traits can still be observed in the later MP group, these are often weakly expressed compared with the earlier MP group (figures 3–5). This is important not just because it definitively rejects the persistent narrative of evolutionary stasis among Pleistocene hominin populations in China. It also serves the foundation for further studies of the dynamic processes that shaped the variability observed

in Middle Pleistocene humans there. With the benefit of an expanded sample and new analytical methods, we have sufficient data to explore hypotheses that move past the persistent 70 year old of models of eastern Eurasian hominin evolution, which have largely been built upon the ideas of Tielhard de Chardin, Movius and others who called the region an evolutionary backwater [28,30,101]. In addition, exploring the reasons for this pattern within a biogeographical framework should be a top priority for research in the region. Expanding on these relationships and interpreting results with a deep understanding of local processes (e.g. [102]) is an essential part of improving palaeoanthropological paradigms and moving beyond an outdated interpretive framework. We hope that further studies will reveal the relationship between human-environment interactions and evolutionary processes in eastern Eurasia and the roles theses played in human evolution there.

Data accessibility. This article has no additional data.

Authors' contributions. W.L. and X.W. designed the research. W.L., X.W. and S.X. collected data. W.L., S.A., X.W. and S.X. analysed data. W.L., S.A., S.X. and X.W. wrote the paper.

All authors gave final approval for publication and agreed to be held accountable for the work performed therein.

Competing interests. We declare we have no competing interests.

Funding. This study has been supported by the Strategic Priority Research Program of Chinese Academy of Sciences (XDB26000000), and National Natural Science Foundation of China (41630102, 41872030).

Acknowledgements. We thank colleagues and students who have assisted with this study.

References

1. Weidenreich F. 1943 *The skull of* Sinanthropus pekinensis*: a comparative study on a primitive hominid skull*, 484p. Pehpei, Chungking: Geological Survey of China.
2. Weidenreich F. 1936. Mandible of *Sinanthropus pekinensis*: a comparative study. In *Palaeontologica sinica*, pp. 1–132. *New Series* D 5 № 1. Peking, China: The Geological Survey of China.
3. Weidenreich F. 1937 The dentition of sinanthropus pekinensis: a comparative odontography of the hominids. In *Palaeontologica Sinica. New Series D.* № 1. Peking, China: The Geological Survey of China.
4. Wu X, Shang H. 2002 Preliminary study on the variations of *Homo erectus* in China. *Quat. Sci.* **2**, 20–28.
5. Antón SC. 2003 Natural history of *Homo erectus*. *Yearb. Phys. Anthropol.* **46**, 126–170. (doi:10.1002/ajpa.10399)
6. Baab KL. 2010 Cranial shape in Asian *Homo erectus*: geographic, anagenetic, and size-related variation. In *Asian paleoanthropology* (eds CJ Norton, DR Braun), pp. 57–79. Amsterdam, The Netherlands: Springer.
7. Athreya S, Wu X. 2017 A multivariate assessment of the Dali hominin cranium from China: morphological affinities and implications for Pleistocene evolution in East Asia. *Am. J. Phys. Anthropol.* **164**, 679–701. (doi:10.1002/ajpa.23305)
8. Liu W *et al.* 2017 A mandible from the Middle Pleistocene Hexian site and its significance in relation to the variability of Asian *Homo erectus*. *Am. J. Phys. Anthropol.* **162**, 715–731. (doi:10.1002/ajpa.23162)
9. Wu X-J *et al.* 2019 Archaic human remains from Hualongdong, China, and Middle Pleistocene human continuity and variation. *Proc. Natl Acad. Sci. USA* **116**, 9820–9824. (doi:10.1073/pnas.1902396116)
10. Athreya S. 2017 Dead end evolutionary lineage, says the White man: the evolution of *Homo erectus* and *Homo sapiens* in Asia. In *86th Annual Meeting of the American Association of Physical Anthropologists*, p. 104. New Orleans, LA: Wiley.
11. Etler D. 2004 *Homo erectus* in East Asia: human ancestor or evolutionary dead-end? *Athena Rev.* **4**, 37–50.
12. Rightmire GP. 1986 Stasis in *Homo erectus* defended. *Paleobiology* **12**, 324–325. (doi:10.1017/S0094837300013828)
13. Swisher CC, Rink WJ, Antón SC, Schwarcz HP, Curtis GH, Suprijo A. 1996 Latest *Homo erectus* of Java: potential contemporaneity with *Homo sapiens* in southeast Asia. *Science* **274**, 1870–1874. (doi:10.1126/science.274.5294.1870)
14. Weidenreich F. 1939 *Sinanthropus pekinensis* and his significance for the problem of human evolution. *Bull. Geol. Soc. China* **19**, 1–17. (doi:10.1111/j.1755-6724.1939.mp19001001.x)
15. Wu X, Zhang Y. 1978. *Synthetic studiy of fossil humans in China. Collection of papers on paleoanthropology (in Chinese)*. Beijing, China: Science Press.
16. Wolpoff MH, Wu XZ, Thorne AG. 1984. Modern *Homo sapiens* origins: a general theory of hominid evolution involving the fossil evidence from East Asia. In *The origins of modern humans. A world survey of the fossil evidence* (eds FH Smith, F Spencer), pp. 411–483. New York: NY: Alan R Liss.
17. Wu X. 1998 Origin of modern humans of China viewed from cranio-dental characteristics of late *Homo sapiens* in China. *Acta Anthropol. Sin.* **17**, 276–282.
18. Rightmire GP. 1992 *Homo erectus*: ancestor or evolutionary side branch? *Evol. Anthropol.: Issues News Rev.* **1**, 43–49. (doi:10.1002/evan.1360010204)
19. Stringer CB. 2016 The origin and evolution of *Homo sapiens*. *Phil. Trans. R. Soc. B* **371**, 20150237. (doi:10.1098/rstb.2015.0237)
20. Wu X, Poirier FE. 1995 *Human evolution in China: a metric description of the fossils and a review of the sites*. New York: NY: Oxford University Press.
21. Wu L, XiuJie W, Song X. 2014 *Human fossils in China*. Beijing, China: Science Press.
22. Liu W, Schepartz LA, Xing S, Miller-Antonio S, Wu X, Trinkaus E, Martinón-Torres M. 2013. Late Middle Pleistocene hominin teeth from Panxian Dadong, South China. *J. Hum. Evol.* **64**, 337–355. (doi:10.1016/j.jhevol.2012.10.012)
23. Xing S *et al.* 2015. Hominin teeth from the early Late Pleistocene site of Xujiayao, Northern China. *Am. J. Phys. Anthropol.* **156**, 224–240. (doi:10.1002/ajpa.22641)
24. Xing S, Martinón-Torres M, Bermúdez de Castro JM, Zhang Y, Fan X, Zheng L, Huang W, Liu W. 2015 Middle Pleistocene hominin teeth from Longtan Cave, Hexian, China. *PLoS ONE* **9**, e114265. (doi:10.1371/journal.pone.0114265)
25. Cui Y, Wu X. 2015 A geometric morphometric study of a Middle Pleistocene cranium from Hexian, China. *J. Hum. Evol.* **88**, 54–69. (doi:10.1016/j.jhevol.2015.08.001)
26. Li Z-Y, Wu X-J, Zhou L-P, Liu W, Gao X, Nian X-M, Trinkaus E. 2017 Late Pleistocene archaic human crania from Xuchang, China. *Science* **355**, 969–972. (doi:10.1126/science.aal2482)
27. Xing S, Martinón-Torres M, de Castro JMB. 2019 Late Middle Pleistocene hominin teeth from Tongzi, southern China. *J. Hum. Evol.* **130**, 96–108. (doi:10.1016/j.jhevol.2019.03.001)
28. Teilhard de Chardin P. 1941 *Early Man in China*. Peking, China: Institut de Geo-Biologie.
29. Movius HL. 1944 *Early man and pleistocene stratigraphy in southern and Eastern Asia*. Cambridge, MA: Peabody Museum.
30. Movius Jr HL. 1948 The Lower Palaeolithic cultures of Southern and Eastern Asia. *Trans. Am. Philos. Soc.* **38**, 329–420. (doi:10.2307/1005632)
31. Dennell R. 2014 East Asia and human evolution: from cradle of mankind to cul-de-sac. In *Southern Asia, Australia and the search for human origins* (eds R Dennell, M Porr), pp. 8–20. Cambridge, UK: Cambridge University Press.

32. Dennell R. 2016 Life without the Movius Line: the structure of the East and Southeast Asian Early Palaeolithic. *Quat. Int.* **400**, 14–22.
33. Darwin J. 2008 *After Tamerlane: the global history of empire since 1405*. New York, NY: Bloomsbury Publishing USA.
34. Wu X. 2005 Palaeoanthropological and molecular studies on the origin of modern humans in China. *Trans. R. Soc. S. Afr.* **60**, 115–119. (doi:10.1080/00359190509520488)
35. Baab KL. 2008 The taxonomic implications of cranial shape variation in *Homo erectus*. *J. Hum. Evol.* **54**, 827–847. (doi:10.1016/j.jhevol.2007.11.003)
36. Rightmire GP. 2013 *Homo erectus* and Middle Pleistocene hominins: brain size, skull form, and species recognition. *J. Hum. Evol.* **65**, 223–252. (doi:10.1016/j.jhevol.2013.04.008)
37. Kaifu Y, Indriati E, Aziz F, Kurniawan I, Baba H. 2011 Cranial morphology and variation of the earliest Indonesian hominids. In *Asian paleoanthropology* (eds CJ Norton, DR Braun), pp. 143–157. Amsterdam, The Netherlands: Springer.
38. Bailey SE, Liu W. 2010. A comparative dental metrical and morphological analysis of a Middle Pleistocene hominin maxilla from Chaoxian (Chaohu), China. *Quat. Int.* **211**, 14–23. (doi:10.1016/j.quaint.2009.01.008)
39. Wu XJ, Bruner E. 2016. The endocranial anatomy of Maba 1. *Am. J. Phys. Anthropol.* **160**, 633–643. (doi:10.1002/ajpa.22974)
40. Wu XJ, Crevecoeur I, Liu W, Xing S, Trinkaus E. 2014 Temporal labyrinths of eastern Eurasian Pleistocene humans. *Proc. Natl Acad. Sci. USA* **111**, 10 509–10 513. (doi:10.1073/pnas.1410735111)
41. Liu W, Wu X, Xing S. 2019 The morphological evidence for the regional continuity and diversity of Middle Pleistocene human evolution in China. *Acta Anthropol. Sin.* **38**, 473–490.
42. Oppo D, McManus J, Cullen J. 1998 Abrupt climate events 500 000 to 340 000 years ago: evidence from subpolar North Atlantic sediments. *Science* **279**, 1335–1338. (doi:10.1126/science.279.5355.1335)
43. Shi P, Yang T, Tian Q, Jiang S, Fan Z, Wang J. 2013 Loess record of climatic changes during MIS 12–10 in the Jingyuan section, northwestern Chinese Loess Plateau. *Quat. Int.* **296**, 149–159. (doi:10.1016/j.quaint.2012.08.2102)
44. Wu N, Chen X, Rousseau D, Li F, Pei Y, Wu B. 2007 Climatic conditions recorded by terrestrial mollusc assemblages in the Chinese Loess Plateau during marine oxygen isotope stages 12–10. *Quat. Sci. Rev.* **26**, 1884–1896. (doi:10.1016/j.quascirev.2007.04.006)
45. Grove M. 2014 Evolution and dispersal under climatic instability: a simple evolutionary algorithm. *Adapt. Behav.* **22**, 235–254. (doi:10.1177/1059712314533573)
46. Santoro S, Green AJ, Figuerola J. 2013 Environmental instability as a motor for dispersal: a case study from a growing population of glossy ibis. *PLoS ONE* **8**, e82983. (doi:10.1371/journal.pone.0082983)
47. Grove M, Lamb H, Roberts H, Davies S, Marshall M, Bates R, Huws D. 2015 Climatic variability, plasticity, and dispersal: a case study from Lake Tana, Ethiopia. *J. Hum. Evol.* **87**, 32–47. (doi:10.1016/j.jhevol.2015.07.007)
48. Dennell RW, Martinón-Torres M, Bermúdez de Castro JM. 2011 Hominin variability, climatic instability and population demography in Middle Pleistocene Europe. *Quat. Sci. Rev.* **30**, 1511–1524. (doi:10.1016/j.quascirev.2009.11.027)
49. Ao H *et al*. 2020 Two-stage mid-Brunhes climate transition and mid-Pleistocene human diversification. *Earth Sci. Rev.* **210**, 103354. (doi:10.1016/j.earscirev.2020.103354)
50. Chen TM, Zhou LP. 2009 Dating of the Peking Man site: a comparison between existing chronology and the $^{26}Al/^{10}Be$ burial ages. *Acta Anthropol. Sin.* **28**, 285–291.
51. Xing S, Martinón-Torres M, de Castro JMB. 2018 The fossil teeth of the Peking Man. *Sci. Rep.* **8**, 1–11. (doi:10.1038/s41598-018-20432-y)
52. An ZS *et al*. 1990 Magnetostratigraphic sates of Lantian *Homo erectus*. *Acta Anthropol. Sin.* **9**, 1–7.
53. Xing S, Sun C, Martinón-Torres M, de Castro JMB, Han F, Zhang Y, Liu W. 2016 Hominin teeth from the Middle Pleistocene site of Yiyuan, eastern China. *J. Hum. Evol.* **95**, 33–54. (doi:10.1016/j.jhevol.2016.03.004)
54. Guo Y *et al*. 2019 $^{26}Al/^{10}Be$ burial dating of the Middle Pleistocene Yiyuan hominin site, Shandong Province, Noerthn China. *Sci. Rep.* **9**, 6961. (doi:10.1038/s41598-019-43401-5)
55. Wu R, Dong X. 1982 Preliminary study of *Homo erectus* remains from Hexian, Anhui. *Acta Anthropol. Sin.* **1**, 2–13.
56. Grün R *et al*. 1998 ESR and U-series analyses of teeth from the palaeoanthropological site of Hexian, Anhui Province, China. *J. Hum. Evol.* **34**, 555–564. (doi:10.1006/jhev.1997.0211)
57. Zhou CL *et al*. 1999 Discussion of Nanjing Man's age. *Acta Anthropol. Sin.* **18**, 255–262.
58. Wu RK, Xingxue L, Xinzhi W, Xinan M. 2002 *Homo erectus from Nanjing*. Nanjing, China: Jiangsu Science and Technology Publishing House.
59. Yin GM *et al*. 2002 Chronology of the stratum containing the skull of the Dali Man. *Chin. Sci. Bull.* **47**, 1302–1307. (doi:10.1360/02tb9289)
60. Wu X, Athreya S. 2013 A description of the geological context, discrete traits, and linear morphometrics of the Middle Pleistocene hominin from Dali, Shaanxi Province, China. *Am. J. Phys. Anthropol.* **150**, 141–157. (doi:10.1002/ajpa.22188)
61. Wu RK. 1988 The reconstruction of the fossil human skull from Jinniushan, Yingkou, Liaoning Province and its main features. *Acta Anthropol. Sin.* **7**, 97–101.
62. Chen TM, Yang Q, Wu E. 1993 Eletron spin resonance dating of teeth enamel samples from Jinniushan palaeoanthropological site. *Acta Anthropol. Sin.* **12**, 337–346.
63. Woo JK, Peng RC. 1959 Fossil skull of early paleoanthropic stage found at Mapa, Shaoguan, Kwangtung Province. *Vertebrata PalAsiatica* **3**, 176–182.
64. Shen GJ *et al*. 2014 Age of Maba hominin site in southern China: evidence from U-series dating of Southern Branch Cave. *Quat. Geochronol.* **23**, 56–62. (doi:10.1016/j.quageo.2014.06.004)
65. Yuan SX, Chen TM, Gao SJ. 1986 Uranium series chronological sequence of some palaeolithic sites in south China. *Acta Anthropol. Sin.* **5**, 179–190.
66. Wu XJ *et al*. 2012 Nasal floor variation among eastern Eurasian Pleistocene *Homo*. *Anthropol. Sci.* **120**, 217–226. (doi:10.1537/ase.120709)
67. Shen GJ, Lin JH. 1991 U-series age of Yanhuidong cave, the site of Tongzi Man. *Acta Anthropol. Sin.* **10**, 65–72.
68. Shen GJ *et al*. 2010 Mass spectrometric U-series dating of the Chaoxian hominin site at Yinshan, eastern China. *Quat. Int.* **211**, 24–28. (doi:10.1016/j.quaint.2009.02.020)
69. Chen TM, Yuan SX, Gao SJ. 1984 The study on Uranium series dating of fossil bones and an absolute age sequence for the main Paleolithic sites of north China. *Acta Anthropol. Sin.* **3**, 259–269.
70. Wu XJ, Trinkaus E. 2014 The Xujiayao 14 mandibular ramus and Pleistocene *Homo* mandibular variation. *C.R. Palevol* **13**, 333–341. (doi:10.1016/j.crpv.2013.10.002)
71. Li Z *et al*. 2014 Study on stratigraphic age, climate changes and environment background of Houjiayao Site in Nihewan Basin. *Quat. Int.* **349**, 42–48. (doi:10.1016/j.quaint.2014.06.003)
72. Ao H *et al*. 2017 An updated age for the Xujiayao hominin from the Nihewan Basin, North China: implications for Middle Pleistocene human evolution in East Asia. *J. Hum. Evol.* **106**, 54–65. (doi:10.1016/j.jhevol.2017.01.014)
73. Wang FG, Li F. 2020 Discussions on stratigraphy and age of the Xujiayao Hominin. *Acta Anthropol. Sin.* **39**, 161–172.
74. Jones HL, Rink WJ, Schepartz LA, Miller-Antonio S, Weiwen H, Hou Y-M, Wang W. 2004 Coupled electron spin resonance (ESR)/uranium-series dating of mammalian tooth enamel at Panxian Dadong *J. Archaeol. Sci.* **31**, 965–977. (doi:10.1016/j.jas.2003.12.010)
75. Martin R, Saller K. 1957 *Lehrbuch der anthropologie*. Stuttgart, Germany: Fischer.
76. Howells WW. 1973 Cranial Variation in Man: A Study by Multivariate Analysis of Patterns of Difference Among Recent Human Populations. *Papers of the Peabody Museum, Harvard University* **67**.
77. Wayman JC. 2003 Multiple imputation for missing data: what is it and how can I use it? In *Annual Meeting of the American Educational Research Association*, Chicago, IL.
78. Yuan YC. 2000 Multiple imputation for missing data: concepts and new developments. In *Proceedings of the Twenty-Fifth Annual SAS Users Group International Conference Paper No. 267–25*. Cary, NC: SAS Institute.

79. Schafer JL. 1999 Multiple imputation: a primer. *Stat. Methods Med. Res.* **8**, 3–15. (doi:10.1177/096228029900800102)
80. Darroch J, Mossiman J. 1985 Canonical and principal components of shape. *Biometrika* **72**, 241–252. (doi:10.1093/biomet/72.2.241)
81. Athreya S, Glantz MM. 2003 Impact of character correlation and variable groupings on modern human population tree resolution. *Am. J. Phys. Anthropol.* **122**, 134–146. (doi:10.1002/ajpa.10220)
82. Wu X, Braüer G. 1993 Morphological comparison of archaic *Homo sapiens* crania from China and Africa. *Zeit. Morph. Anthropologie* **79**, 241–259. (doi:10.1127/zma/79/1992/241)
83. Athreya S. 2006 Patterning of geographic variation in Middle Pleistocene *Homo* frontal bone morphology. *J. Hum. Evol.* **50**, 627–643. (doi:10.1016/j.jhevol.2005.11.005)
84. Athreya S. 2009 A comparative study of frontal bone morphology among Pleistocene hominin fossil groups. *J. Hum. Evol.* **57**, 786–804. (doi:10.1016/j.jhevol.2009.09.003)
85. Liu W, Zhou M, Xing S. 2018 Occurrence of Carabelli's cusp in Chinese hominins and its evolutionary implication. *Acta Anthropol. Sin.* **37**, 159–175.
86. Rightmire GP. 2004 Brain size and encephalization in early to Mid-Pleistocene *Homo*. *Am. J. Phys. Anthropol.* **124**, 109–123. (doi:10.1002/ajpa.10346)
87. Rosenberg KR, Zune L, Ruff C. 2006 Body size, body proportions, and encephalization in a Middle Pleistocene archaic human from northern China. *Proc. Natl Acad. Sci. USA* **103**, 3552–3556. (doi:10.1073/pnas.0508681103)
88. Ruff C, Trinkaus E, Holliday T. 1997 Body mass and encephalization in Pleistocene *Homo*. *Nature* **387**, 173–176. (doi:10.1038/387173a0)
89. Van Valen L. 1965 Morphological variation and width of ecological niche. *Am. Nat.* **99**, 377–390. (doi:10.1086/282379)
90. Kolbe JJ, Glor RE, Rodriguez Schettino L, Lara AC, Larson A, Losos JB. 2004 Genetic variation increases during biological invasion by a Cuban lizard. *Nature* **431**, 177. (doi:10.1038/nature02807)
91. Grove M. 2015 Palaeoclimates, plasticity, and the early dispersal of *Homo sapiens*. *Quat. Int.* **369**, 17–37. (doi:10.1016/j.quaint.2014.08.019)
92. Grove M. 2017 Environmental complexity, life history, and encephalisation in human evolution. *Biol. Philos.* **32**, 395–420. (doi:10.1007/s10539-017-9564-4)
93. Ash J, Gallup GG. 2007 Paleoclimatic variation and brain expansion during human evolution. *Human Nature* **18**, 109–124. (doi:10.1007/s12110-007-9015-z)
94. Sun Y *et al.* 2019 Diverse manifestations of the mid-Pleistocene climate transition. *Nat. Commun.* **10**, 352. (doi:10.1038/s41467-018-08257-9)
95. Ge J, Deng C, Wang Y, Shao Q, Zhou X, Xing S, Pang H, Jin C. 2020 Climate-influenced cave deposition and human occupation during the Pleistocene in Zhiren Cave, southwest China. *Quat. Int.* **559**, 14–23. (doi:10.1016/j.quaint.2020.01.018)
96. Xijun N *et al*. 2021. Massive cranium from Harbin in northeastern China establishes a new Middle Pleistocene human lineage. *Innovation* **2**, 100130. (doi:10.1016/j.xinn.2021.100130)
97. Potts R. 1998 Variability selection in hominid evolution. *Evol. Anthropol.: Issues News Rev.* **7**, 81–96.
98. Chang C-H *et al*. 2015 The first archaic *Homo* from Taiwan. *Nat. Commun.* **6**, 6037. (doi:10.1038/ncomms7037)
99. Chen F-H *et al*. 2019 A late Middle Pleistocene Denisovan mandible from the Tibetan plateau. *Nature* **569**, 409–412. (doi:10.1038/s41586-019-1139-x)
100. Zhang D-J *et al*. 2020. Denisovan DNA in Late Pleistocene sediments from Baishiya Karst Cave on the Tibetan plateau. *Science* **370**, 584–587. (doi:10.1126/science.abb6320)
101. Black D, Teilhard de Chardin P, Young CC, Pei WC. 1933 *Fossil man in China: the Choukoutien Cave deposit with a synopsis of our present knowledge of the late Cenozoic in China*. Beijing, China: Geological Survey of China and the Section of Geology of the National Academy of Beijing.
102. Kaifu Y, Aziz F, Indriati E, Jacob T, Kurniawan I, Baba H. 2008 Cranial morphology of Javanese *Homo erectus*: new evidence for continuous evolution, specialization, and terminal extinction. *J. Hum. Evol.* **55**, 551–580. (doi:10.1016/j.jhevol.2008.05.002)